PHYSICAL REVIEW D **71,** 104016 (2005)

Accuracy requirements for the calculation of gravitational waveforms from coalescing compact binaries in numerical relativity

Mark Miller

Jet Propulsion Laboratory, California Institute of Technology, Pasadena, California 91109, USA
(Received 21 February 2005; published 13 May 2005)

I discuss the accuracy requirements on numerical relativity calculations of inspiraling compact object binaries whose extracted gravitational waveforms are to be used as templates for matched filtering signal extraction and physical parameter estimation in modern interferometric gravitational wave detectors. Using a post-Newtonian point particle model for the premerger phase of the binary inspiral, I calculate the maximum allowable errors for the mass and relative velocity and positions of the binary during numerical simulations of the binary inspiral. These maximum allowable errors are compared to the errors of state-of-the-art numerical simulations of multiple-orbit binary neutron star calculations in full general relativity, and are found to be smaller by several orders of magnitude. A post-Newtonian model for the error of these numerical simulations suggests that adaptive mesh refinement coupled with second-order accurate finite difference codes will *not* be able to robustly obtain the accuracy required for reliable gravitational wave extraction on Terabyte-scale computers. I conclude that higher-order methods (higher-order finite difference methods and/or spectral methods) combined with adaptive mesh refinement and/or multipatch technology will be needed for robustly accurate gravitational wave extraction from numerical relativity calculations of binary coalescence scenarios.

DOI: 10.1103/PhysRevD.71.104016 PACS numbers: 04.25.Dm, 02.60.Cb, 04.30.Db, 04.40.Dg

I. INTRODUCTION

Studies in numerical relativity in the past decades have claimed at least partial motivation from the imminent direct detection of gravitational waves from both ground based (LIGO, GEO, TAMA, VIRGO) and space based (LISA) detectors. Theoretical calculations of gravitational waveforms from realistic astrophysical phenomena will be an essential ingredient in the extraction of characteristic information of gravitational wave sources (e.g., mass, spin, size, and composition of compact objects) from the detected gravitational waves. In particular, gravitational waves produced during the coalescence of binary compact objects (neutron stars and/or black holes) are strong candidates for direct detection, and thus it is precisely these systems that are of great interest to the numerical relativity community. Recent advances in numerical relativity, in particular, with respect to the stability of binary black hole evolutions [1–3] and binary neutron star evolutions [4–6], make possible the calculation of gravitational waves from fully general and consistent numerical relativity simulations of binary coalescences.

However, numerical relativity simulations contain errors that arise from attempting to solve continuum differential equations (the Einstein field equations) on infinite domains (asymptotically flat spacetimes) with digital computers of finite size and speed. Examples of these errors are truncation errors (e.g., due to the truncating of Taylor-series expansions for finite difference methods or to the truncating of function expansions for spectral methods) and boundary errors (e.g., errors induced by the introduction of a computational domain in causal contact with the binary and/or the gravitational waves being emitted). The magnitude of these errors determines the accuracy of the numerical relativity simulation (here, I do not include modeling errors in the determination of the accuracy of a numerical relativity code, e.g., inaccurate equation of state for neutron star matter or astrophysically incorrect initial data for binary simulations). In this paper, I demonstrate, for the first time, a calculation for determining the accuracy required of inspiraling binary numerical relativity simulations in order that the characteristics of the extracted gravitational waveform represent the physics of the binary system to the experimental error level of the gravitational wave detector. Using the gravitational waveform accuracy criterion in [7], I calculate the sensitivity of the gravitational waveform to various parameters of the dynamical binary system (e.g., binary separation, angular velocity, mass) assuming a specific target sensitivity for the gravitational wave detector; forcing the errors in the same dynamical parameters within numerical relativity coalescence simulations to be smaller than these sensitivities will be one way of guaranteeing an extracted theoretical waveform accurate to the sensitivity level of the gravitational wave detector. Truncation and boundary errors in the orbital separation of the multiple-orbit binary neutron star simulations in [4] are calculated and are shown to be several orders of magnitude *larger* than the margin allowed for by the gravitational wave sensitivity calculation. Using a post-Newtonian model of the truncation and boundary errors in the binary neutron star numerical relativity simulations, I estimate the computational resources required for accurate gravitational waveform generation from such simulations, and conclude that both higher-order methods and mesh refinement or multipatch technology will be required for robust, reliable, and accu-

rate gravitational waveform extraction from numerical relativity simulations of coalescing binary inspirals and mergers.

The outline of the rest of the paper is as follows. In Section II, the sensitivity of gravitational waveforms to various physical characteristics of the coalescing binary is calculated for binary black hole and binary neutron star systems. In Section III, I compare these sensitivities to errors in recent state-of-the-art binary simulations in numerical relativity, and find the errors to be orders of magnitude larger than the gravitational wave sensitivities. I conclude by discussing methods that may be helpful in reducing the error of numerical relativity calculations of coalescing binaries to levels that would permit their extracted gravitational waveforms to be used with confidence as templates in modern interferometric gravitational wave detectors.

II. REQUIRED ACCURACY FOR NUMERICAL RELATIVITY SIMULATIONS OF BINARY INSPIRALS: SENSITIVITY OF GRAVITATIONAL WAVEFORMS TO PHYSICAL CHARACTERISTICS OF THE BINARY

In order to calculate the sensitivity of gravitational waveforms to various physical characteristics of the coalescing binary, I calculate binary coalescence solutions to the post-Newtonian equations of motion for nonspinning point particles. This formalism has the advantage that accurate gravitational waveforms can be calculated in astrophysically relevant binary coalescence scenarios. The major disadvantage is that at small binary separations, the point particle approximation breaks down due to finite size effects; the gravitational waveforms obtained by solving the post-Newtonian equations of motion must therefore be truncated at the point where these effects become important. As a result, the sensitivities calculated here will only bound the true sensitivity, i.e. the sensitivity of the entire gravitational wave train, through plunge, merger, and ringdown of the final merged object. In other words, due to the fact that the gravitational waveform is being truncated when finite size effects become important, the sensitivity of the entire physical gravitational waveform to variations in the physical characteristics of the system is being *underestimated*. Thus, the errors in numerical relativity simulations must be *at least as small as* the sensitivities calculated here.

A. Post-Newtonian equations of motion

The general relativistic equations of motion for nonspinning point particles in harmonic coordinates with positions $\vec{x}_1$ and $\vec{x}_2$, and masses m_1 and m_2, can be written in a post-Newtonian expansion as

$$\begin{aligned}\frac{d^2\vec{x}}{dt^2} = &-\frac{m}{r^2}\hat{n} + \frac{m}{r^2}[\hat{n}(A_{1\mathrm{PN}} + A_{2\mathrm{PN}} + A_{3\mathrm{PN}} + \cdots) \\ &+ \dot{r}\,\vec{v}(B_{1\mathrm{PN}} + B_{2\mathrm{PN}} + B_{3\mathrm{PN}} + \cdots)] + \frac{8}{5}\eta\frac{m}{r^2}\frac{m}{r} \\ &\times [\dot{r}\,\hat{n}(A_{2.5\mathrm{PN}} + A_{3.5\mathrm{PN}} + A_{4.5\mathrm{PN}} + \cdots) \\ &- \vec{v}(B_{2.5\mathrm{PN}} + B_{3.5\mathrm{PN}} + B_{4.5\mathrm{PN}} + \cdots)],\end{aligned} \tag{1}$$

where $\vec{x} = \vec{x}_2 - \vec{x}_1$ is the relative separation of the particles, $\vec{v} = \vec{v}_2 - \vec{v}_1$ is the relative velocity between the particles, $r = |\vec{x}|$, $\hat{n} = \vec{x}/r$, $m = m_1 + m_2$, $\eta = m_1 m_2/m^2$, and $\dot{r} = dr/dt$. The post-Newtonian expansion in Eq. (1) is carried out in powers of $\epsilon \sim m/r \sim v^2$ (I set $G = c = 1$), where each power of ϵ represents one post-Newtonian (PN) order in the series. The 1PN and 2PN terms are standard (e.g., see [8–10]). The 2.5PN [9–11] and 3.5PN [10] have also been completely determined. The 3.0PN terms have just recently been calculated [12] up to one gauge-dependent constant. Employing an energy and angular momentum balance technique, the 4.5PN terms have been fixed modulo 12 free ''gauge'' parameters [13] (appendix B of [14] demonstrates that these free parameters have a negligible effect on inspiral dynamics). Once the initial relative positions and velocities of the particles are given, Eq. (1) is then solved numerically for the time evolution of the binary system. Specifically, if the initial separation r and its time derivative $\dot{r}$ along with the initial relative angular position ϕ and its time derivative $\dot{\phi}$ are specified at time $t = 0$, then the equations of motion Eq. (1) specifies $r(t)$ and $\phi(t)$ for $t > 0$ (I assume the binary orbits within the $z = 0$ plane).

I use the post-Newtonian formalism presented in [15–18] to calculate the polarization state $h(t) = h_+(t)$ of the gravitational radiation as a function of the motion of the binary. For definiteness, I fix both observation angles (Φ, Θ) to be 0 for the remainder of the paper (i.e., the binary, which is orbiting in the $z = 0$ plane, is observed along the $+z$-axis).

B. Waveform sensitivity to physical characteristics of the binary

An inner product on the space of waveforms $h(t)$ is defined as

$$\langle h_1|h_2\rangle = 4\,\mathrm{Re}\left\{\int_0^\infty df\,\frac{\tilde{h}_1^*(f)\tilde{h}_2(f)}{S_h(f)}\right\}, \tag{2}$$

where $\tilde{h}_1(f)$ and $\tilde{h}_2(f)$ are the Fourier transforms of the two waveforms $h_1(t)$ and $h_2(t)$, and $S_h(f)$ is the one-sided power spectral density of the strain noise of the detector. For the calculations in the remainder of this paper, the model of the one-sided power spectral density of the strain noise for the advanced LIGO detector found in [19] is used for $S_h(f)$, where the mass scale is set by assuming an equal-mass binary with $m_1 = m_2 = 1.4M_\odot$. The latest

detection rates for binary neutron star coalescences for the advanced LIGO sensitivity is between 40 and 650 events per year [20]. Assume that the gravitational waveform $h(t)$ contains an error $\delta h(t)$. Arguments in [7] determine the criteria that the error $\delta h(t)$ be small enough so that the quantity

$$\Delta \equiv \frac{1}{2} \frac{\langle \delta h | \delta h \rangle}{\langle h | h \rangle} \tag{3}$$

satisfies

$$\Delta \leq 0.01. \tag{4}$$

This accuracy criteria is based on matched filtering accuracy arguments, physical parameter estimation arguments, and arguments based on the total information content of the gravitational wave signal (see [7] for details). The specific criteria Eq. (4) is based on the assumption that the signal to noise ratio is of order 10. Much higher signal to noise ratios are expected for LISA, and therefore an even more stringent requirement on $\delta h(t)$ could be required in that case (e.g., for gravitational wave templates used in physical parameter estimation, the required Δ scales like the inverse square of the signal to noise ratio).

Using the post-Newtonian equations of motion described in Sec. II A as a model for coalescing binary compact objects, along with the gravitational wave accuracy requirements Eqs. (3) and (4), I now analyze the sensitivity of the gravitational waveform to various physical characteristics of the binary dynamics. Note that the gravitational waveform $h(t)$ of our post-Newtonian model of a binary inspiral depends solely on the 8 parameters $\vec{\lambda} = \{r_0, \phi_0, \dot{r}_0, \dot{\phi}_0, m_1, m_2, t_f, R\}$. Here, r_0 and ϕ_0 specifies the relative binary position at the initial time $t = t_0$, $\dot{r}_0$ and $\dot{\phi}_0$ specifies the initial relative binary velocity, m_1 and m_2 specifies the mass of each compact object, while R specifies the observation distance from the center of mass of the binary. The parameter t_f is the time at which the waveform is truncated due to the breakdown of the post-Newtonian point particle approximation. This breakdown occurs when the internal structure of the individual compact objects has a significant effect on the orbital dynamics of the binary. Throughout the rest of this paper, I take t_f to be the time at which the binary separation $r(t_f) = 4m$ for equal-mass binary black holes and $r(t_f) = 8m$ for equal-mass binary neutron stars. I orient the system such that the initial relative angle $\phi_0 = 0$. For a specific initial binary separation r_0, I set the initial relative velocity parameters $\dot{r}_0$ and $\dot{\phi}_0$ to be those specified by the unique *quasicircular solution* of the binary (the quasicircular solution to the PN equations of motion is obtained by starting from circular orbit initial data in the limit as the initial separation $r \to \infty$, see Sec. 2 of [14]).

For a specific set of parameters $\vec{\lambda}$ that specify the waveform $h(t)$, define the quantity $\Delta_{0.01}\vec{\lambda}$ to be the ranges in the parameters such that the change in the gravitational waveform $\delta h(t)$ induced by separately changing each individual component λ_i satisfies $\Delta \leq 0.01$. The quantity $\Delta_{0.01}\vec{\lambda}$ can be interpreted as the "allowable" error in each parameter during the course of a numerical relativity time evolution simulation, since changes within this range do not appreciably (to the tolerance set by Eq. (3)) affect the gravitational waveform.

As a concrete example, I examine the sensitivity of the gravitational waveform on changes in the binary separation r. I solve the 4.5PN equations of motion for the quasicircular solution for an equal-mass ($m_1 = m_2 = m/2$) binary and find that exactly 3 orbits before merger (for definiteness, assume binary black holes and define the merger to be at binary separation $r = 4m$), the binary separation is $r = 7.3195m$, the relative radial velocity is $\dot{r} = -0.005\,573$, and the relative angular velocity is $\dot{\phi} = 0.042\,63/m$. Using these values of parameters as initial data, the subsequent gravitational waveform $h(t)$ for the last 3 orbits before merger is computed. I define a second gravitational waveform $h'(t)$ to be the one obtained by changing the initial binary separation $r_0 \to r_0 + \delta r$, keeping all other initial parameters fixed. The change in the waveform $\delta h(t)$ induced by changing the initial binary separation an amount δr is therefore $\delta h(t) = h'(t) - h(t)$. The quantity Δ (Eq. (3)) can now be calculated; in Fig. 1, the quantity Δ is plotted as a function of the change in initial binary separation δr. The quantity $\Delta_{0.01} r$ is defined as the range of δr such that $\Delta \leq 0.01$; in this case, $\Delta_{0.01} r = 0.0165m$ (see Fig. 1). The intuitive interpretation of this calculations is as follows: δr represents the error in the binary separa-

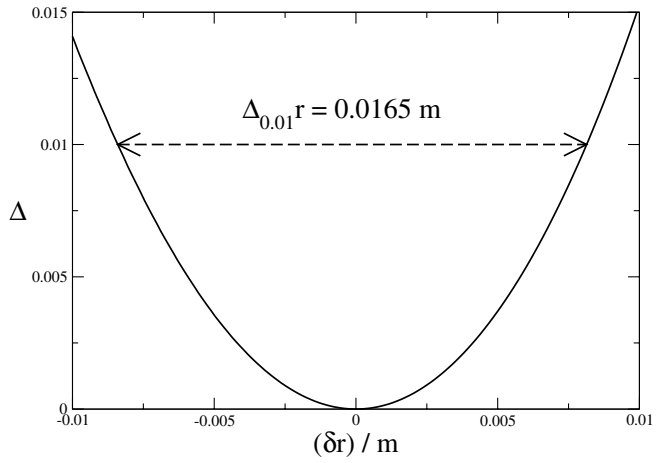

FIG. 1. An example of the definition of the $\Delta_{0.01}$ operator. Δ (Eq. (3)) is plotted as a function of the variation of the initial orbital separation δr for an equal-mass black hole binary, starting 3 orbits before merger (m is the total mass of the system). In order that variations in the resulting gravitational waveform satisfy $\Delta < 0.01$, any variation in the initial orbital separation r must satisfy $\delta r < 0.0165m$. I therefore define $\Delta_{0.01} r = 0.0165m$.

tion of a numerical relativity simulation of equal-mass black holes at a time when 3 orbits remain until the merger. The quantity $\Delta_{0.01} r$ represents the allowable error in binary separation r as set by the tolerance level of Eq. (4). Thus, a numerical error $|\delta r|$ in the binary separation of a numerical relativity simulation at a time when 3 orbits remain until merger that is greater than $\Delta_{0.01} r$ would correspond to an unacceptable level of error in that simulation.

In Fig. 2, the parameter tolerance $\Delta_{0.01}\lambda_i$ for physical parameters m_1, m_2, r_0, $\dot{\phi}_0$ and $\dot{r}_0$ is plotted as a function of the number of orbits until merger for equal-mass binary black holes and binary neutron stars. Note that the gravitational waveform is roughly an order of magnitude more sensitive to small changes in the angular velocity as compared to small changes in the radial velocity.

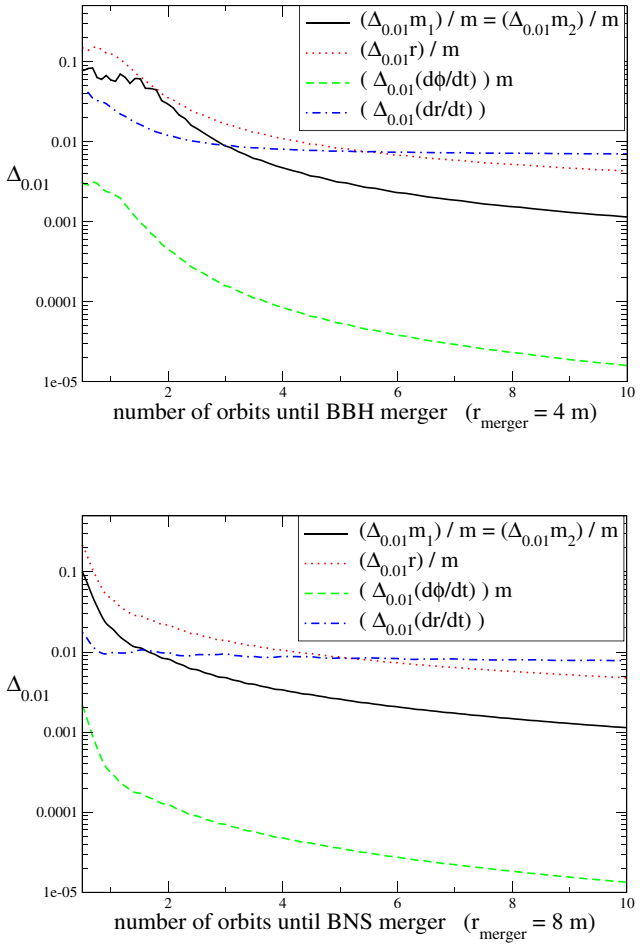

FIG. 2 (color online). Gravitational wave sensitivities to various dynamical quantities for orbiting binary black holes (top panel) and binary neutron stars (lower panel) are plotted as a function of the number of orbits remaining until merger. Shown are gravitational wave sensitivities of the mass of each compact object ($\Delta_{0.01} m_1 = \Delta_{0.01} m_2$, solid line), the orbital separation ($\Delta_{0.01} r$, dotted line), the relative orbital angular velocity ($\Delta_{0.01}\dot{\phi}$, dashed line), and the relative orbital radial velocity ($\Delta_{0.01}\dot{r}$, alternating dot-dashed line).

III. CASE STUDY: BINARY NEUTRON STAR EVOLUTION

A. Comparing errors in numerical relativity simulations of coalescing binary neutron stars to gravitational waveform sensitivities

Several recent studies [4,6] have analyzed various aspects of orbiting binary neutron stars by performing 3 + 1 general relativistic hydrodynamic simulations. It is instructive to analyze the accuracy of these simulations in comparison to the sensitivity required for the accurate generation of gravitational waves as represented in Fig. 2.

In [4], quasiequilibrium initial data sets corresponding to two equal-mass, corotating binary neutron stars were numerically evolved using a general 3 + 1 numerical relativity code that simultaneously solved the Einstein field equations coupled to the general relativistic hydrodynamics equations. In order to assess the quality of the numerical solution, the exact same initial data set was numerically evolved 5 separate times, using a variety of discretization parameters and outer boundary placements (see Table II in [4]). There are two types of numerical errors associated with the simulations presented in [4]. The first type of numerical error is due to the finite difference approximation, where derivatives in the partial differential equations have been replaced by truncated Taylor-series approximations. Assuming that the finite difference equations used in [4] are consistent and stable, Lax convergence theorems (see [21]) state that the relationship between any quantity Q constructed from a true solution of the differential equation is related to that same quantity observed in the numerical solution $Q_{\text{numerical}}$ by

$$Q = Q_{\text{numerical}} + C_1(\Delta x) + C_2(\Delta x)^2 + \cdots, \qquad (5)$$

where C_i are constants (which are different for distinct quantities Q) and Δx is the discretization parameter used in the construction of the finite difference equations. Assuming that Δx is made small enough so that higher-order terms can be ignored, define the truncation error $(\Delta Q)_{\text{trunc}}$ of the calculations in [4] to be

$$(\Delta Q)_{\text{trunc}} = C_1(\Delta x) + C_2(\Delta x)^2. \qquad (6)$$

While the code being analyzed is formally second-order convergent in both space and time, the use of high resolution shock capturing (HRSC) methods renders the hydrodynamics convergence rate to be first order in space in regions where the dynamical variables obtain a local extrema (see, e.g., [22]). Thus, the form of the truncation error, Eq. (6), necessarily contains a term proportional to the first power of the spatial discretization parameter Δx.

The second type of numerical error that exists in the simulations presented in [4] is due to the location of the boundary of the computational domain. Ideally, the computational domain would be placed many gravitational wavelengths away from center of mass of the orbiting

binary, thus minimizing the effect of the boundary on the dynamics of the binary. However, computational resource limitations coupled with the fact that the code used in [4] is only second-order accurate and does not employ adaptive mesh refinement, prevented the location of the outer boundary of the computational domain to be placed no farther than 1/4 of a gravitational wavelength from the center of mass of the system. I model the error associated with the close proximity of the boundary of the computational domain analogously with that of the truncation error; assume that the error in any particular quantity Q induced by the boundary goes to 0 as the distance between the center of mass of the system and the location of the outer boundary (denote this distance as r_b) goes to infinity. I expand this boundary-induced error, $(\Delta Q)_{\rm bound}$, as a power series about $r_b = \infty$ and assume that the values of r_b used in the calculations in [4] are large enough so that the power series can be truncated as

$$(\Delta Q)_{\rm bound} = \frac{B_1}{r_b} + \frac{B_2}{r_b^2} \tag{7}$$

The total numerical error, therefore, is represented as the relationship between the exact quantity $Q_{\rm exact}$ specified from the solution to the differential equations and quantity $Q_{\rm numerical}$ produced by numerical simulations:

$$Q_{\rm exact} = Q_{\rm numerical} + (\Delta Q)_{\rm trunc} + (\Delta Q)_{\rm bound}. \tag{8}$$

I now compare the errors in the binary separation r contained in the simulations of [4] with the sensitivity of the gravitational waveform to changes in the binary separation, $\Delta_{0.01} r$. I use Eq. (8) to calculate the numerical errors in the calculation of the binary separation $r(t)$ for the simulations presented in [4]. At each time t, I assume that the numerically computed binary separation $r_{\rm numerical}$ takes the form of Eq. (8):

$$r_{\rm exact} = r_{\rm numerical} + (\Delta r)_{\rm trunc} + (\Delta r)_{\rm bound}. \tag{9}$$

Using the results from the five simulations displayed in Fig. 17 in [4] (which are reproduced in Fig. 4 of this paper), the five unknowns in Eq. (9) ($r_{\rm exact}$, C_1, C_2, B_1, and B_2) are specified at each time t. The absolute values of the truncation error $(\Delta r)_{\rm trunc}$ and the boundary error $(\Delta r)_{\rm bound}$ of the binary separation are plotted in Fig. 3. For comparison, the gravitational wave sensitivity to binary separation, $\Delta_{0.01} r$ (see Fig. 2), is also plotted. Important to notice is the magnitude of the errors (both truncation errors and boundary errors) in the binary separation of the numerical relativity calculations in [4] as compared to the sensitivity of the gravitational waveform to the binary separation: the simulation errors in the binary separation are several orders of magnitude larger than the gravitational waveform sensitivity to variations in the binary separation! Assuming that they are to be used as signal detection and parameter estimation templates, the gravitational waveforms extracted from these numerical simulations will contain errors that dominate the experimental errors in modern interferometric gravitational wave detectors. Steps must be taken to improve the accuracy of these simulations before gravitational waves extracted from them can be considered for use as templates in gravitational wave detectors.

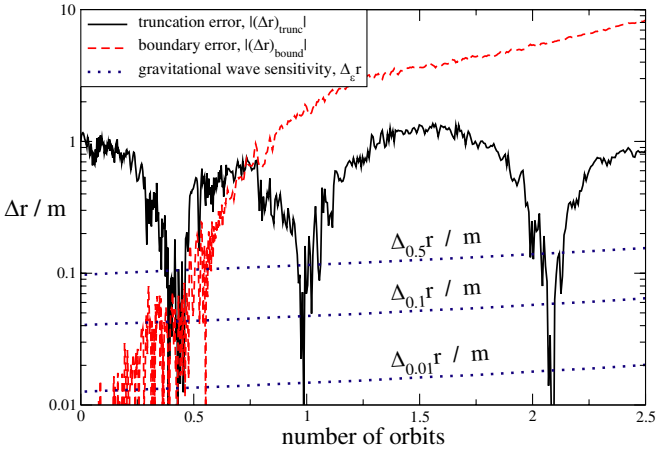

FIG. 3 (color online). The absolute value of the truncation error $(\Delta r)_{\rm trunc}$ and boundary error $(\Delta r)_{\rm bound}$ of the orbital separation is plotted as a function of the number of orbits for the binary neutron star simulations in [4]. For comparison, the gravitational wave sensitivity to variations in the orbital separation, $\Delta_\epsilon r$ is also plotted. Assuming the use of gravitational waveforms produced from numerical simulations as matched filtering search templates in a gravitational wave detector, sensitivities of $\Delta_{0.01}$, $\Delta_{0.1}$, and $\Delta_{0.5}$ correspond to a detector event loss rate of 3%, 27%, and 87%, respectively.

B. Estimating the accuracy and computational resources required to extract sufficiently accurate waveforms from binary coalescence simulations

In order to obtain information on the computational resources required to reduce the boundary and truncation errors of simulations such as those in [4] down to acceptable levels (i.e., such that the errors in the gravitational waveforms δh induced by these numerical errors satisfy $\Delta \leq 0.01$), these errors and their effect on gravitational waveforms are modeled using the post-Newtonian equations of motion for spinless point particles, Eq. (1). The same mass and initial orbital separation is used in the post-Newtonian model as was used in the numerical relativity simulations. The initial angular velocity of the binary is determined by the circular orbit assumption (see [14]), which is consistent with the initial data used for the numerical relativity simulations in [4]. In order to model the effects of truncation and boundary errors with the post-Newtonian model, it is modified in the following way. First, the initial angular velocity of the binary is set to be a function of discretization Δx and outer boundary placement r_b as

$$\dot{\phi}_0(\Delta x, r_b) = \dot{\phi}_{\rm circular} + \sigma_1\left(\frac{\Delta x}{m}\right) + \sigma_2\left(\frac{\Delta x}{m}\right)^2 + \sigma_3\left(\frac{m}{r_b}\right) + \sigma_4\left(\frac{m}{r_b}\right)^2 \tag{10}$$

where $\dot{\phi}_{\rm circular}$ is the angular velocity determined by the circular orbit assumption. Second, the post-Newtonian equations of motion are modified so that the evolution of the angular momentum is given by

$$\left(\frac{dL}{dt}\right) = \left(\frac{dL}{dt}\right)_{\rm PN} + \sigma_5\left(\frac{\Delta x}{m}\right) + \sigma_6\left(\frac{\Delta x}{m}\right)^2 + \sigma_7\left(\frac{m}{r_b}\right) + \sigma_8\left(\frac{m}{r_b}\right)^2 \tag{11}$$

In the ideal limit of infinite resolution ($\Delta x \to 0$) and infinite distance from the center of mass of the system to the computational boundaries ($r_b \to \infty$), the solutions to these modified post-Newtonian equations reduce to the standard post-Newtonian inspiral solutions starting with circular orbit initial data. The constants σ_1 through σ_8 are to be chosen so as to best reproduce the effects of the truncation errors and boundary errors from the multiple-orbit simulations of binary neutron stars in [4]. To this end, I define an "error function" $\chi(\sigma_i)$, which measures the difference in the orbital separation profile in time between the 5 numerical relativity simulations NS-A through NS-E from [4] (which I denote as $r^j_{\rm nr}(t)$, $j = 1, 2, 3, 4, 5$) and the solution to the modified post-Newtonian equations Eqs. (1), (10), and (11) (which I denote as $r_{\rm pn}(t, \Delta x, r_b, \sigma_i)$), as

$$\chi(\sigma_i) = \frac{1}{5}\sum_{j=1}^{5}\sqrt{\frac{\int_0^{t_f} dt (r_{\rm pn}(t, (\Delta x)_j, (r_b)_j, \sigma_i) - r^j_{\rm nr}(t))^2}{\int_0^{t_f} dt}} \tag{12}$$

where $(\Delta x)_j$ and $(r_b)_j$ are the discretization and boundary placement parameters used to produce the numerical relativity result $r^j_{\rm nr}(t)$ for each of the five multiple-orbit numerical relativity simulations of binary neutron stars performed in [4]. The time integrations in Eq. (12) use $t_f = 610m$, which corresponds to roughly 2.5 orbits of the binary system. A global minimum of $\chi(\sigma^{\rm min}_i) = 0.093m$ is found numerically by varying the σ_i parameters. A comparison among the five numerical relativity simulations NS-A through NS-E from [4] and the solutions of the modified post-Newtonian equations of motion Eqs. (1), (10), and (11) using the $\sigma^{\rm min}_i$ parameters that minimize $\chi(\sigma_i)$ is shown in Fig. 4.

Using the solutions to the modified post-Newtonian equations of motion corresponding to parameters $\sigma^{\rm min}_i$ that minimize $\chi(\sigma_i)$ as a model for the effects of the truncation and boundary errors in the full numerical relativity simulations of orbiting binary neutron stars in [4], I am now able to gauge the effect these errors have on the resulting gravitational waveform. Specifically, the goal is

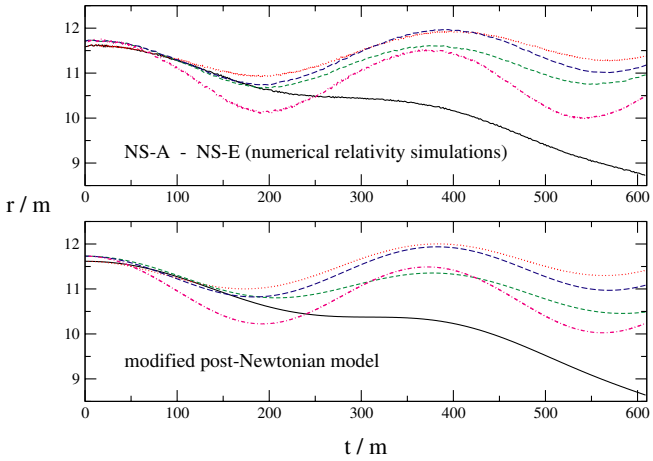

FIG. 4 (color online). Top panel: plotted is the orbital separation as a function of time from the numerical relativity simulations of orbiting binary neutron stars in [4]. These simulations were performed with the same initial data, but with different discretization parameters Δx and computational domain boundary placement parameters r_b. Shown are simulations NS-A (solid line), NS-B (dotted line), NS-C (short dashed line), NS-D (long dashed line), and NS-E (alternating dot-dashed line), evolved to time $t = 610m$, which corresponds to 2.5 orbits. Bottom panel: the modified post-Newtonian model $r_{\rm pn}(t, (\Delta x)_j, (r_b)_j, \sigma^{min}_i)$ is plotted for the five discretization and boundary parameters $\{(\Delta x)_j, (r_b)_j\}$, $(j = 1, 2, 3, 4, 5)$, corresponding to the parameters used in numerical relativity simulations NS-A through NS-E, respectively. The modified post-Newtonian model robustly encapsulates the effects of the truncation and boundary errors within the full numerical relativity simulations.

to find bounds on the discretization parameter Δx and outer boundary location parameter r_b such that the error in the produced gravitational waveform satisfies, e.g., Eq. (4). In order to calculate $\Delta \equiv (1/2)\langle \delta h | \delta h \rangle / \langle h | h \rangle$, I take the target gravitational waveform $h(t)$ to be that determined by the solution to the modified post-Newtonian equations of motion in the limit as $\Delta x \to 0$ and $r_b \to \infty$, which is just the waveform obtained from the ordinary post-Newtonian equations of motion assuming initial data corresponding to a circular orbit. This waveform we denote as $h_0(t)$. The "error" in the waveform $\delta h(t)$ induced by the truncation error and boundary error in the numerical simulations can then be calculated as

$$\delta h(t, \Delta x, r_b) = h(t, \Delta x, r_b) - h_0(t) \tag{13}$$

where $h(t, \Delta x, r_b)$ is the waveform obtained by the modified post-Newtonian equations of motion using discretization parameter Δx and boundary placement parameter r_b (and, of course, using the σ_i parameters that minimizes $\chi(\sigma_i)$). Figure 5 is a plot of the target waveform $h_0(t)$ and the waveform $h(t, \Delta x_{\rm NS-A}, r_{b\rm NS-A})$, which corresponds to the best numerical relativity simulation NS-A (the solid line in Fig. 4).

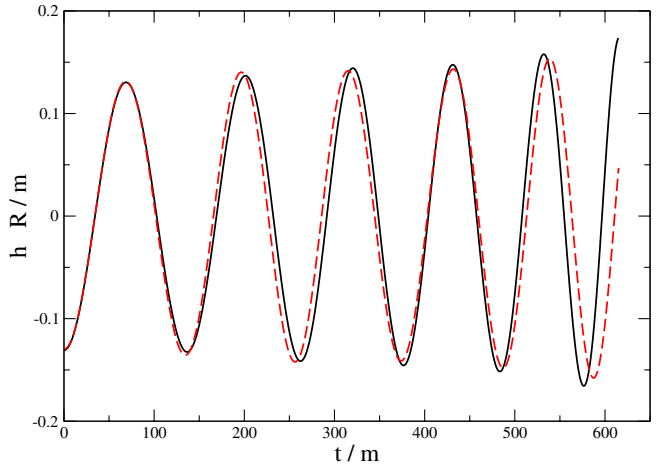

FIG. 5 (color online). Gravitational waveforms (multiplied by the distance to the source, R). The solid line waveform corresponds to $h_0(t)$, which is the "zero error" waveform corresponding to the modified post-Newtonian solution with discretization parameter $\Delta x = 0$ and boundary placement parameter $r_b = \infty$. The dashed line waveform is $h(t, \Delta x_{\mathrm{NS-A}}, r_{b\mathrm{NS-A}})$, which corresponds to the numerical relativity simulation NS-A (see Fig. 4). The difference between these waveforms (Eq. (13)) corresponds to $\Delta = 0.054$, which is 5 times larger than our target accuracy (see Eqs. (3) and (4)).

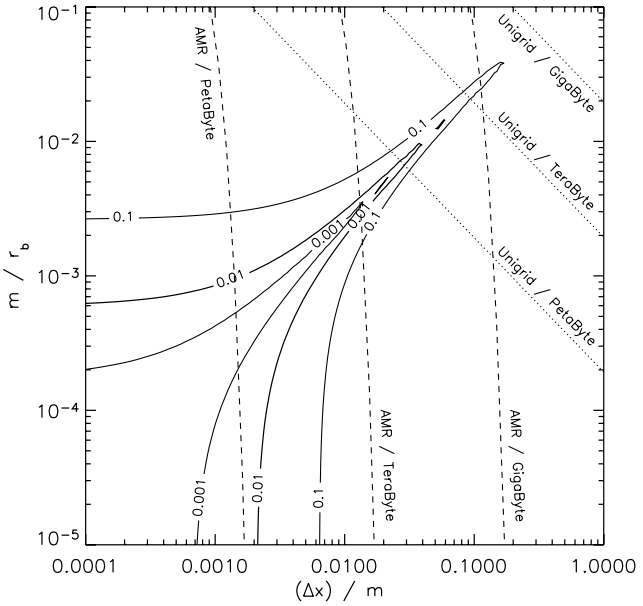

FIG. 6. Contour plots of the gravitational wave accuracy parameter Δ (Eq. (3)) as a function of discretization parameter Δx and distance from the center of mass of the binary to the computational domain boundary r_b for the numerical relativity simulations of binary neutron stars in [4]. Configurations for various sized computers with a unigrid code and an AMR code (nested boxes, with grid refinement ratio of 2) is shown for reference.

Shown in Fig. 6 is a contour plot of Δ (Eq. (3)) as a function of Δx and r_b. Contours for $\Delta = 0.1$, 0.01, and 0.001 are shown. The "peninsula"-like shape of the contours in Fig. 6 are due to the slightly offsetting effect of the truncation and boundary errors in the numerical simulations of [4]; larger discretization parameters Δx tend to artificially increase the rate at which angular momentum is lost from the binary, while closer outer boundary placements (smaller r_b) tend to have the opposite effect. For reference, the computational memory resources for the *unigrid* numerical relativity code used in [4] is shown in Fig. 6, indicating Gigabyte (1024^3 bytes), Terabyte (1024^4 bytes), and Petabyte (1024^5 bytes) requirements. Adaptive mesh refinement (AMR) allows the efficient minimization of errors induced by the boundary by permitting the placement of the boundary of the computational domain farther from the coalescing binary for a fixed amount of computational resources (other methods could also reduce boundary errors, such as employing a Cauchy-characteristic matching code [23] or using a null-approaching slicing far from the center of mass of the binary [24]). The computational memory resources for an AMR version of the code is also shown in Fig. 6 (I have assumed that the finest resolution grid is the size of the compact objects, that the grid at each level has the same computational volume as every other grid, and that the grids are uniformly nested with a refinement ratio of 2).

An optimistic reading of Fig. 6 implies that numerical relativity simulations using a 10 Terabyte computer would be able to attain the target accuracy of $\Delta = 0.01$. However, the reliability and robustness of such a calculation would be highly questionable, due to the fact that the discretization and boundary placement would have to be fine-tuned to reach the tip of the $\Delta = 0.01$ contour peninsula in Fig. 6. In order to obtain a robustly accurate simulation from which gravitational waveforms could be extracted with confidence, it will likely be necessary to, at a minimum, use a target resolution $\Delta x_{\mathrm{target}}$ and boundary placement $r_{b\mathrm{target}}$ such that the gravitational wave accuracy parameter Δ (Eq. (3)) satisfies $\Delta \leq 0.01$ for all $\Delta x \leq \Delta x_{\mathrm{target}}$ and $r_b \geq r_{b\mathrm{target}}$. From Fig. 6, we see that this minimum target configuration is at roughly $\Delta x_{\mathrm{target}} \sim 0.002m$ and $r_{b\mathrm{target}} \sim 2000m$. However, this minimum target configuration would not be possible with a unigrid code, and would just barely be possible with an AMR code on a *Petabyte* machine, although the execution time of such a simulation would render it highly impractical. In order to reduce the computational resources required to perform sufficiently accurate inspiral calculations in numerical relativity, higher-order methods will need to be employed in future calculations. Possible higher-order extensions to the code in [4] include the use of spectral methods (where the truncation error drops off exponentially with the number of collocation points) or the use of higher-order finite difference methods. Figure 7 reproduces the results of Fig. 6 assuming that the truncation error of the simulation falls off as $(\Delta x)^8$, which is consistent with using an eighth-

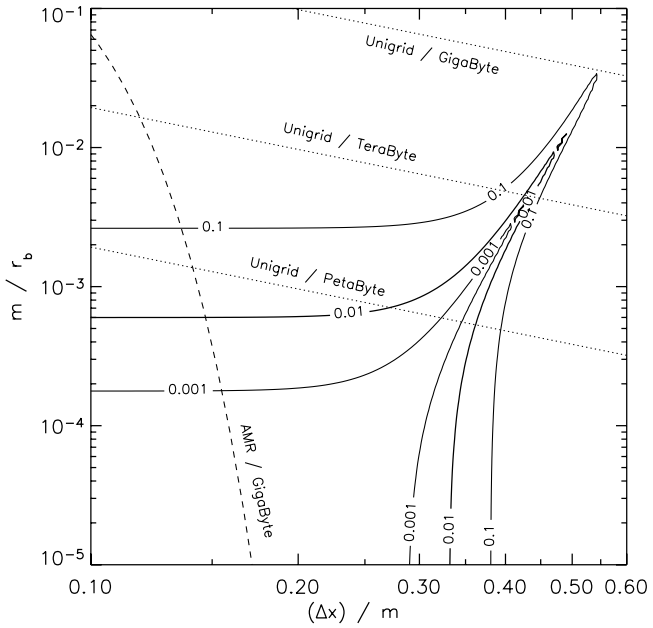

FIG. 7. Contour plots of Δ (Eq. (3)) as a function of discretization parameter Δx and distance from the center of mass of the binary to the computational domain boundary r_b, assuming an eighth-order finite difference method is used for the numerical relativity simulations of binary neutron stars. Configurations for various sized computers with a unigrid code and an AMR code is shown for reference. Note that higher-order finite difference methods, couple with AMR, will be able to robustly obtain the required gravitational waveform accuracy $\Delta \leq 0.01$ on Gigabyte computers.

order finite difference method. The increased accuracy of the eighth-order method allows for a larger discretization parameter Δx; the new minimum target discretization is $\Delta x_{\mathtt{target}} \sim 0.33m$. As seen in Fig. 7, a combination of both higher-order finite difference methods and AMR will yield a robustly accurate simulation on Gigabyte scale computers. Not only will the memory fingerprint of a sufficiently accurate simulation be relatively small for an AMR code employing higher-order methods, but just as importantly, the execution time of a simulation using such a code will be considerably smaller than, e.g., the 200 000 CPU hours required for the NS-A simulation from [4] displayed in Fig. 4.

C. Generality of results

Various aspects of the implementation of numerical relativity simulations of coalescing binary compact objects, including details regarding the spacetime and hydrodynamics solvers, boundary conditions, initial data, gauge conditions, and total evolution times, could have a large impact on the details of the accuracy studies presented in sections III A and III B. For instance, the implementation of constraint-preserving boundary conditions [25,26] in the simulations presented in [4] could reduce by a significant amount the errors in the simulation induced by the outer boundaries. Of course, any approximation method employed in the generation of gravitational wave templates used for signal searches and parameter estimations in gravitational wave detectors must be validated; one must directly confirm that the approximation is good relative to the signal to noise ratio of the detector. As such, the calculations presented in sections III A and III B are a *demonstration* for the case of numerical relativity simulations of coalescing binary compact objects; gravitational waveform results from different numerical relativity codes using different methods and/or different implementation techniques must be validated in a similar way.

It is instructive to compare the accuracy requirements found here with other multiple-orbit binary neutron star simulation results, such as those in [6]. However, the detailed accuracy studies of numerical relativity binary simulations in sections III A and III B are made possible by repeating the same simulation (more specifically, using the same initial data) many times using a wide variety of discretization parameters and outer boundary placements, as presented in [4]. While the simulations presented in [6] used several discretization parameters and boundary placements, they were performed for differing initial data corresponding to an array of initial binary separations. Thus, the detailed studies in sections III A and III B cannot be repeated using the results from the multiple-orbit neutron star simulations presented in [6]. However, a casual inspection of the simulations from [6] confirms that the errors induced by the boundary are similar to those of [4]. In Fig. 8, a simulation of initially corotating binary neutron stars from [6] is displayed; the coordinate separation of the neutron stars is plotted as a function of time over two orbital periods. The equations of state used in the simulations of [4,6] are identical, and the results from [6] plotted in Fig. 8 use neutron stars that are 7% more massive than those used in [4]. Note that the simulation from [6] (labeled ''Stable'' in Fig. 1 of reference [6]) displayed in the top panel in Fig. 8 has an initial separation of $r_i = 9.85M_0$ (separation values in [6] are normalized by the total baryonic mass M_0; we follow this convention in Fig. 8 and during the discussion here). After two orbits, the binary separation has *increased* over 10%, while a post-Newtonian point particle simulation using identical mass, initial separation, circular orbit initial conditions, and accurate to order $(v/c)^9$ in the post-Newtonian expansion, predicts that the separation should instead *decrease* by 15% during the first two orbits (the post-Newtonian simulation is plotted along side the Stable simulation from [6] in the top panel of Fig. 8). At the very least, it is clear that the separation of the neutron stars cannot increase, due to the fact that i) the dissipative effects of gravitational radiation will cause a decrease in the binary separation and ii) while the circular orbit initial condition induces a slight eccentricity to the orbit of the binary, this initial condition

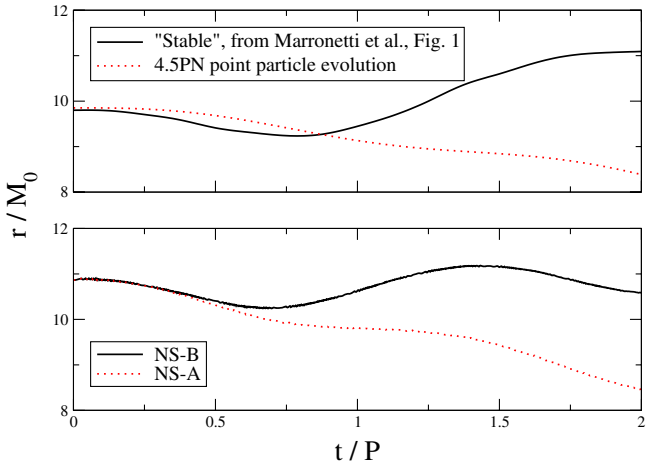

FIG. 8 (color online). Top panel: the separation of binary neutron stars (normalized by the total baryonic rest mass of the system M_0) simulated by the general relativistic hydrodynamics code in [6] is plotted as a function of time for two orbital periods. For comparison, the solution to the post-Newtonian point particle equations of motion (accurate to order $(v/c)^9$) for the same masses and initial conditions is shown. Bottom panel: the binary separation from the general relativistic simulations NS-A and NS-B in [4] (also shown in Fig. 4 using a different normalization) is plotted for two orbital periods. NS-B has a similar outer boundary placement as that used in the simulations of [6], but NS-A has an outer boundary that is located twice as far away from the binary as that of simulation NS-B. The similarity of the top and bottom panels suggests that the unphysical *increase* in the binary separation of the Stable simulation in [6] is due to boundary errors, and that the magnitude of the errors are roughly the same for the simulations in [4,6].

corresponds to an apastron (maximum separation) point in the dynamical evolution [14]. To compare with the simulations analyzed in this paper, the simulations NS-A and NS-B from [4] shown in Fig. 4 are reproduced in the lower panel of Fig. 8. Simulation NS-B has a similar outer boundary placement as that used in the Stable simulation from [6], but NS-A has an outer boundary that is twice the distance from the binary as compared to NS-B. The similarities between the top and bottom panels of Fig. 8 suggests that the cause of the unphysical increase in the binary separation during the first two orbits of the Stable simulation from [6] is the close proximity of the boundary of the computational domain, and that the errors induced by the boundary of the computational domain in [4,6] are of a similar magnitude.

IV. CONCLUSIONS

Using a criterion for gravitational waveform template accuracy motivated by matched filtering and parameter estimation requirements of modern interferometric gravitational wave detectors, I have calculated the accuracy required of numerical relativity simulations of coalescing compact binary systems. I have calculated the numerical errors of state-of-the-art numerical relativity simulations of orbiting binary neutron stars [4], and I find these errors to be several orders of magnitude larger than the allowed errors determined from gravitational waveform accuracy considerations. Using a post-Newtonian model for the truncation errors and boundary errors in the numerical simulations of [4], the computational resources required in order that these simulations attain an accuracy needed for reliable gravitational wave extraction have been calculated. I find that while mesh refinement technology will provide an improvement over the unigrid second-order accurate simulations of [4], higher-order methods will also be required for a robustly accurate numerical relativity calculation of multiple-orbit binary coalescence calculations on Terabyte-scaled (or smaller) digital computers.

ACKNOWLEDGMENTS

It is a pleasure to thank my colleagues, both at the Jet Propulsion Laboratory and in the California Institute of Technology numerical relativity group, for many useful discussions and suggestions; special thanks to David Meier for his many useful suggestions regarding this manuscript. This research was performed at the Jet Propulsion Laboratory, California Institute of Technology, under contract with the National Aeronautics and Space Administration, funded through the internal Research and Technology Development program. Computational resource support has been provided by the JPL Institutional Computing and Information Services, the NASA Directorates of Aeronautics Research, Science, Exploration Systems, and Space Operations, and NSF NRAC project MCA02N022.

[1] B. Brügmann, W. Tichy, and N. Jansen, Phys. Rev. Lett. **92**, 211101 (2004).
[2] M. Alcubierre, B. Brügmann, P. Diener, F. S. Guzmán, I. Hawke, S. Hawley, F. Herrmann, M. Koppitz, D. Pollney, E. Seidel *et al.*, gr-qc/0411149.
[3] S. Brandt, R. Correll, R. Gómez, M. F. Huq, P. Laguna, L. Lehner, P. Marronetti, R. A. Matzner, D. Neilsen, J. Pullin*et al.*, Phys. Rev. Lett. **85**, 5496 (2000).
[4] M. Miller, P. Gressman, and W.-M. Suen, Phys. Rev. D **69**, 064026 (2004).

[5] M. Shibata and K. Uryu, Prog. Theor. Phys. **107**, 265 (2002).
[6] P. Marronetti, M. Duez, S. Shapiro, and T. Baumgarte, Phys. Rev. Lett. **92**, 141101 (2004).
[7] Éanna É. Flanagan and S. A. Hughes, Phys. Rev. D **57**, 4566 (1998).
[8] T. Damour and N. Deruelle, Phys. Lett. A **87**, 81 (1981).
[9] Y. Itoh, T. Futamase, and H. Asada, Phys. Rev. D **63**, 064038 (2001).
[10] M. E. Pati and C. M. Will, Phys. Rev. D **65**, 104008 (2002).
[11] L. Blanchet, G. Faye, and B. Ponsot, Phys. Rev. D **58**, 124002 (1998).
[12] L. Blanchet and B. Iyer, Classical Quantum Gravity **20**, 755 (2003).
[13] A. Gopakumar, B. Iyer, and S. Iyer, Phys. Rev. D **55**, 6030 (1997).
[14] M. Miller, Phys. Rev. D **69**, 124013 (2004).
[15] R. Epstein and R. V. Wagoner, Astrophys. J. **197**, 717 (1975).
[16] R. V. Wagoner and C. M. Will, Astrophys. J. **210**, 764 (1976).
[17] M. Turner and C. M. Will, Astrophys. J. **220**, 1107 (1978).
[18] C. W. Lincoln and C. M. Will, Phys. Rev. D **42**, 1123 (1990).
[19] Éanna É. Flanagan and S. A. Hughes, Phys. Rev. D **57**, 4535 (1998).
[20] V. Kalogera, C. Kim, D. Lorimer, M. Burgay, N. D'Amico, A. Possenti, R. Manchester, A. Lyne, B. Joshi, M. McLaughlin *et al.*, Astrophys. J. Lett. **614**, L137 (2004).
[21] B. Gustafsson, H.-O. Kreiss, and J. Oliger, *Time Dependent Problems and Difference Methods* (Wiley, New York, 1995).
[22] C. Hirsch, *Numerical Computation of Internal and External Flows* (Wiley-Interscience, New York, 1992).
[23] N. T. Bishop, R. Gómez, L. Lehner, and J. Winicour, Phys. Rev. D **54**, 6153 (1996).
[24] S. Husa, Lect. Notes Phys. **604**, 239 (2002).
[25] O. Sarbach and M. Tiglio, gr-qc/0412115.
[26] L. Kidder, L. Lindblom, M. Scheel, L. Buchman, and H. Pfeiffer, gr-qc/0412116.